Sensors and Materials, Vol. 11, No. 4 (1999) 233–246
MYU Tokyo

S & M 0368

Characterization of Flexible Sapphire Fibers in High-Temperature Pyrometers

Jörg Philipp Kottmann* and Christian Stenzel**

Dornier GmbH, D-88039 Friedrichshafen, Germany

(Received August 31, 1998; accepted March 1, 1999)

Key words: temperature measurement, high temperature, optical fiber thermometry, sapphire sensor, optical fibers

The technique of fabricating high-temperature sensors consisting of flexible sapphire fibers is described. Characterization tests with these sensors, aiming at the determination of the effective aperture, the lower detection limit, the short-term stability, and the effect of scattered light on the temperature signal, have been performed. The tests reveal a high performance of these sensors, which is comparable to that of a sensor made of a rigid sapphire rod. The effective aperture of the flexible fibers has been determined to be slightly larger than that for a rigid sensor (11° compared to 7°). This has been discussed in terms of an increased number of crystal defects near the tip caused by the grinding process.

1. Introduction

Pyrometric temperature measurement relies on the detection of emitted light from the measured object in a distinct infrared wavelength range. In conventional pyrometry the object is optically imaged onto the detector which converts the detected light into an electrical signal. Using Planck's law, the measured radiation density can be converted electronically into a temperature signal. The main set of drawbacks to conventional pyrometry are the need for optical access to the object to be measured, and for the prevention of contamination of the detector or other optical components at elevated temperatures caused by outgassing of heated components.[1]

*Current affiliation: Laboratory of Field Theory and Microwave Electronics, Swiss Federal Institute of Technology, CH-8092 Zürich
**Corresponding author: Dornier GmbH, Department RIO 41, D-88039 Friedrichshafen

These drawbacks can be partially overcome by using optical fibers for transmitting the emitted light to the detector. The fibers can be routed through the furnace to provide a direct optical access to the object. The problem of contamination still exists, but only in a very localized region of the fiber tip.

The optical fiber thermometer (OFT) has been commercially available for about ten years. This system consists of a rigid sapphire rod, a conventional waveguide (quartz fiber), and measuring electronics.[2] The electronics unit includes a silicon photodetector, transimpedance amplifiers, a 16-bit analog-to-digital converter, and a microprocessor.[3] Both the sapphire rod system and the flexible quartz fiber system provide transmission of the emitted IR radiation intensity to the detector. The sapphire fiber is thereby located in areas with an elevated temperature, whereas the quartz fiber is applied for transmission through cold regions. The transmitted radiation density in the wavelength region between 930 nm and 970 nm is converted into the corresponding temperature signal according to Planck's law. This system has been successfully used in numerous high-temperature applications, such as the exact determination of the melting point of several metals, high-precision furnace regulation, and fast thermometry in engines.[3,4]

The time constant of the measurement is only limited by the dynamic range of the electronics, and above the temperature of 1,100°C, a resolution better than ± 0.1°C is achieved. However, during the first years of operation, the following setbacks for particular applications have been identified.

—The routing of the fibers requires straight lines with only one 90° bend feasible.

—The bent region in particular tends to break due to internal mechanical tensions in the sapphire fiber.

On replacing the rigid fibers by flexible ones, these problems could be partially circumvented. Whereas single-crystalline rigid sapphire sensors are commercially available for many years,[5,6] the production of flexible, as well as single-crystalline, sapphire fibers with a diameter of about 300 μm has become possible since the last few years on an industrial basis.[7,8] Several high-temperature applications for sapphire fibers are reported in the literature, for example, as an interferometric strain sensor,[9,10] or as a fiber-optic high-temperature sensor using the birefringence property of sapphire.[11]

However nothing has been reported so far on the feasibility of making an OFT sensor using a flexible fiber with a high performance comparable to that of conventional, rigid ones. It is possible to bend these fibers with a minimum bending radius of 60 mm. Hence, the objectives of this presented work were to investigate the feasibility of fabricating OFT sensors using flexible sapphire fibers and to study their characteristics with respect to the following:

- effective aperture which governs the local resolution of the sensor,
- temperature range, particularly the minimum detectable temperature,
- short-term stability, and
- influence of the light entering the fiber sideways on the temperature signal.

To achieve these objectives, three flexible OFT light pipe sensors with different lengths have been fabricated from bare sapphire rods with a diameter of 325 μm. The light pipe sensor has a flat polished forefront, and ideally, only the radiation which enters the fiber within the angle of acceptance via the forepart is transmitted throughout the fiber to the

detector.

In the following section, the manufacturing procedure for the sensors will be described and afterwards, the experimental setup for the characterization tests and the results of the above-mentioned tests will be reported.

2. Preparation of Flexible Sensors

An OFT sensor consists of the single-crystalline sapphire fiber mounted in a ferrule which fits into a commercial optical coupler. To provide a well-defined aperture, both ends of the fiber should be as smooth as possible. The technology for fabricating an OFT sensor using a flexible fiber is rather similar to the procedure applied to a rigid one. The steps which have been carried out are given below in detail.

—First of all, as an initial preparation, the ends of the fiber are ground using a diamond saw. The side of the saw is used as a grinding sheet.

—To carry out sanding and polishing of both ends, the fiber is glued in a ferrule with a hole of a diameter of 350 μm, using optical glue. This particular glue is quite hard at room temperature but has a low melting point which allows easy removal of the finished fiber from the ferrule after polishing.

—Sanding is carried out using a SiC sheet with 3 μm particles. After the first step described above, it is necessary to sand about 0.2 mm of the end over an estimated duration of 2 h.

—After cleaning, the end is polished with an Al_2O_3 sheet with 0.3 μm particles for a duration of about 15 min.

—After each major step and finally after polishing, the quality of the smoothness of the end is checked using an optical microscope.

—By heating the ferrule to 90°C, the fiber can be removed and cleaned. The steps described above must be carried out on the other end of the fiber. Since one end will normally remain in the ferrule, epoxy, instead of optical glue, can be used to fix the fiber.

3. Characterization Tests

For the characterization tests, three flexible 325 μm sensors with different lengths were fabricated and tested. For comparison, a conventional, commercial rigid light pipe sensor with a diameter of 1.27 mm was used. The lengths of the flexible sensors were 50 mm, 150 mm and 420 mm, while the length of the rigid sensor was 275 mm.

In the first step, the four sensors were calibrated in front of a black-body radiator operating at a temperature of 900°C against the control thermocouple of the radiator. The sensors were positioned consecutively at the same position and the sensor factors adjusted to match the operation temperature of the black-body radiator. To calculate the radiation density from the measured temperature, Planck's law was integrated numerically in the respective wavelength region.

3.1 *Effective aperture*

The aperture is defined as half the acceptance angle α within which the sensor detects light, and the effective aperture means the half-acceptance angle for the complete sensor system including the sapphire fiber, the waveguide, and all optical interfaces up to the measuring unit which could also influence the acceptance angle. Besides the distance of the sensor from the object, the effective aperture governs the local spatial resolution of the sensor. For physical objects, the ideal assumptions of linear optics may not hold and therefore the effective aperture must be determined by measurement.

The experimental setup used to determine this quantity is shown in Fig. 1. At a distance of 9 cm, the sensor faces the center of a large radiation bulb with a diameter of 11.5 cm. The diameter d of the diaphragm and the distance x of the sensor from the diaphragm determine the angle of acceptance via the equation

$$\alpha = \arctan[(d - t)/2x)] \tag{1}$$

with t being the thickness of the sensor. In order to guarantee proper measurement, the light source must illuminate the diaphragm homogeneously. For the large radiation bulb, this was verified in a preparatory measurement.

The radiation density was measured as a function of x for a constant diaphragm diameter d of 8 mm. Since x can be converted into α via eq. (1), the dependence of the detected radiation density from the angle of incidence α is graphically represented in Fig. 2 for the respective sensor types. The maximum density, i.e., the density without the diaphragm, was normalized to unity. These measurements were performed for the three flexible sensors and also for the rigid one using the same optical coupler, waveguide, and measuring channel in the electronic unit. In order to check the reproducibility, these

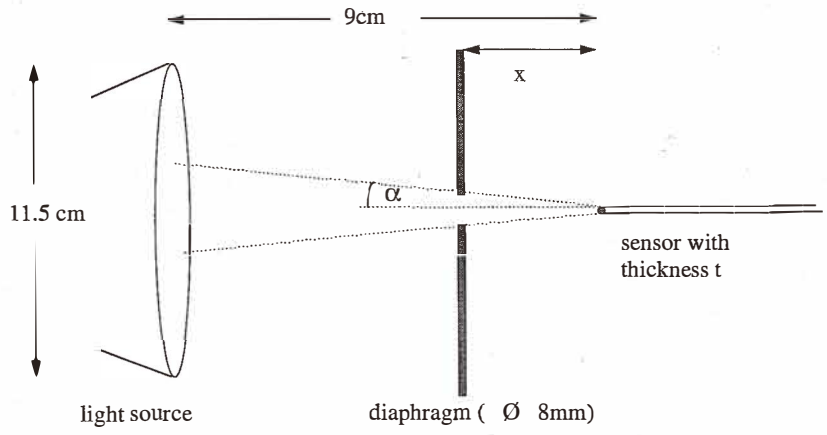

Fig. 1. Experimental setup for the measurement of the effective aperture.

measurements were repeated several times for each sensor. The resulting total error for the determination of the effective aperture, including all systematic errors and the reproducibility, was deduced to be $\Delta\alpha_0 = \pm 0.5°$.

As is seen in Fig. 2, there is a qualitative difference in the curves among the flexible sensors on the one side and the conventional rigid sensor on the other. In order to quantify this difference the effective aperture α_0 is defined as the angle within which 90% of the total radiation intensity is detected. The values of these effective apertures are shown in Table 1. The apertures of the flexible sensors are in the range between 10° and 11°, while the aperture of the rigid sapphire fiber was determined to be 7°. The aperture of the rigid sensor is therefore comparable with the numeric aperture of $NA_{eff} = 0.11$ (6°), as reported by the manufacturer of the sapphire fibers.[12] For the rigid sensor, nearly 90% of the transmitted radiation density is detected within this angle. In contrast, for the flexible sensors, nearly 30% of the radiation density is detected outside this angle. In particular, as seen in Fig. 2, about 5% of the radiation density is still transmitted for angles larger than 15°. This can be recognized with the naked eye as a halo. The cause of that effect may arise in the grinding/polishing procedure and is further discussed in section 3.4.4.

3.2 *Lower temperature range*

Since the flexible sensor transmits less light than the rigid one due to its smaller cross section (ratio of 1:15), the lowest temperature at which the transmitted radiation intensity is sufficient for a proper measurement must be clarified. The electronic unit limits the processing to signals which correspond to temperatures higher than 500°C.

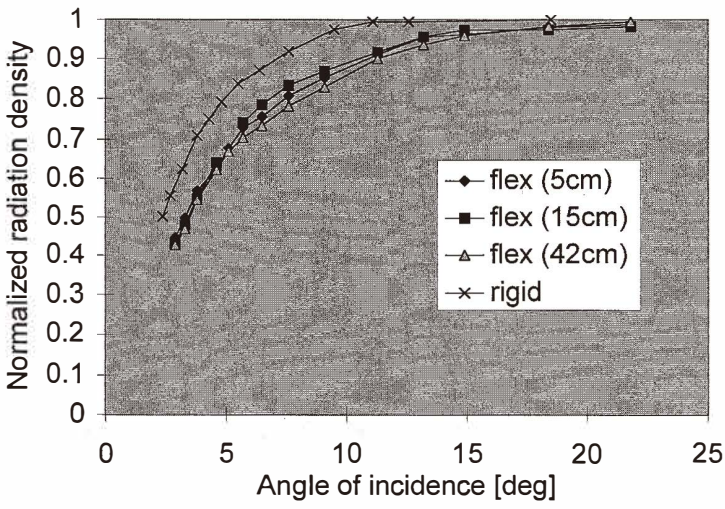

Fig. 2. Measured normalized radiation density versus angle of incidence for different sensors.

Table 1
Effective apertures of the investigated OFT sensors.

	Effective aperture α_0 (± 0.5°)
Rigid light pipe sensor	7.0°
Flexible 50 mm sensor	10.8°
Flexible 150 mm sensor	10.5°
Flexible 420 mm sensor	11.0°

In order to study the behavior of both types of sensors in the lower temperature range, the course of temperature for a heated pipe that was being cooled was measured for the flexible and the rigid sensors, both facing the same spot of the radiation source. No difference in the characteristics of the curve could be seen and no cutoff could be observed down to the boundary of 500°C.

This verifies that for the flexible fiber with a diameter of 325 μm, a sufficient amount of IR light is transmitted and converted to a temperature signal at least down to 500°C. This observation is in good agreement with the fact that the ratio of the calibration factors for the flexible and rigid sensors (1:2.25) does not reflect the ratio of the cross sections. The reason for this is the cross section of the quartz waveguide which is much smaller than the diameter of 1.27 mm of the rigid sensor. To conclude, the limitation for the transmission of IR light throughout the sensor is not the cross section of the sapphire rod in the case of the rigid sensor, but the diameter of the waveguide in this case. Hence, it seems reasonable that the electronics can easily handle an intensity loss by a factor of 2 down to a range which corresponds to 500°C.

3.3 *Short-term stability*

In order to use OFT sensors as control sensors for a high-performance temperature control system, a fast response time and a good short-term stability are needed. Since the response time for a measurement is limited only by the photoelectric effect in the detector, the effective response time of the complete measurement setup is governed by the time constant of the electronic unit. In the actual case, it was set to 25 Hz.

The temperature fluctuations of a noncontrolled radiation source were measured and compared, over a time period of several minutes, with those of a flexible sensor and a rigid OFT sensor. No difference concerning the short-term stability for both sensors could be detected. The overall time resolution for both sensors was determined by the electronic unit and the data-taking system. The short-term stability for both types is comparable and sufficient for high-performance furnace regulation.

3.4 *Effect of scattered light on temperature signal*

3.4.1 *Motivation*

In the section concerning the determination of the effective aperture, a light source which emitted light with nearly constant intensity within an angle of 25° was used, and for larger angles, the intensity rapidly decreased. However, for the application as a furnace control sensor, the sapphire fiber is often routed through zones which are hotter than the measured object, or it ends in a cavity with a temperature gradient. In both cases, parasitic radiation enters the sensor via its sides and may be scattered at crystal defects or refracted at surface imperfections at an angle where the fiber transmits light to the detector. This effect is expected to be much larger for the flexible OFT than for the rigid one, because the defect rate of the flexible fiber is much larger than that for a rigid sapphire rod. The influence of the scattered light is therefore of great interest since it might lead to a reduction of the local resolution or a falsification of the "true" temperature signal.[13]

3.4.2 *Experimental setup*

Two experiments were carried out to investigate the effect of light coupled into the fiber via the side of the fiber. In the first experiment, a high-pressure Xe lamp is focused, with the help of a collimator and a lens from the side, under a fixed angle onto the sensor as sketched in Fig. 3. The sensor itself was directly facing a radiation source in order to provide a constant bias signal which is well above the detection threshold of 500°C. The additional, parasitic radiation density which is coupled into the fiber from the Xe lamp has been determined as a function of the x position.

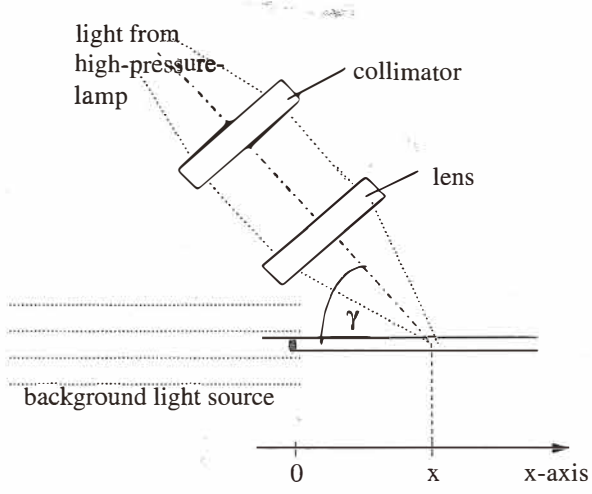

Fig. 3. Sketch of the experimental setup for determining the dependence of scattered light on the angle of incidence with a focused radiation source.

In the second step the dependence of the scattered light on the angle of incidence was investigated. Here, the lens was removed, resulting in parallel incidence of the light from the Xe lamp over a length of 15 mm, as seen in Fig. 4. Using this setup, the parasitic radiation density which was transmitted through the fiber was measured for different angles of incidence.

It should be stressed that no difference in the behavior of the various flexible sensors could be observed and therefore the discussion below generally concerns the flexible sensor.

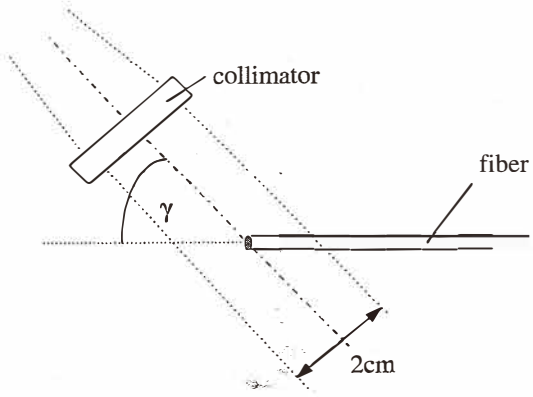

Fig. 4. Sketch of the experimental setup for determining the dependence of scattered light on the angle of incidence with parallel incident light.

3.4.3 *Results*

For the first experiment described above, the measurement data for $\gamma = 90°$ are graphically represented in Fig. 5. The curves for both the flexible and the rigid sensor operating with the same calibration factor are shown. The area under the curve represents the radiation intensity that would be detected by the sensor if a homogeneously extended light source were to illuminate the sensor from the side. It is obvious that most of the light enters the fiber in the region near the tip. In this area the flexible sensor receives about 5 times more intensity than the rigid one.

It should be stressed that the curve in this diagram represents the convolution of the intensity curve of the focus and the absorption function of the fiber for the respective angle in the x direction. It could be shown in another measurement that the width of the tip peak in Fig. 5 represents mostly the intensity curve of the focus in the x direction and not the absorption curve around the tip. The width of the absorption peak was estimated to be on the order of less than 1 mm and therefore this structure could not be resolved.

To gain more information about the effect off the side of the tip, the intensity curve for the flexible sensor in the region 3 cm $< x <$ 8 cm is shown in Fig. 6 for angles of $\gamma = 90°$ and

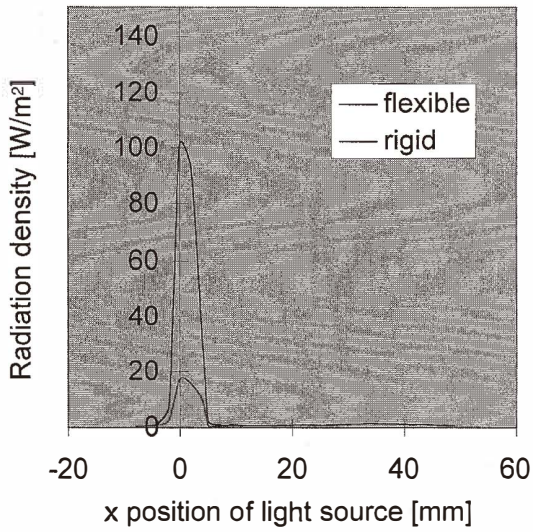

Fig. 5. Intensity of scattered radiation at 90° versus x position of the light source.

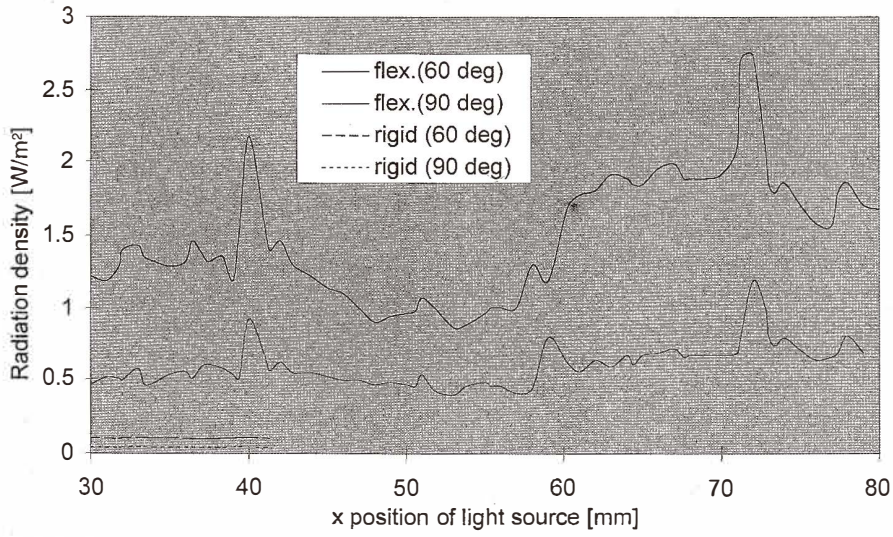

Fig. 6. Detected radiation intensity of scattered light for x positions off the side of the tip ($x = 0$) for two angles of incidence (γ= 60°, 90°) and for two types of investigated sensors.

$\gamma = 60°$. The curves in Fig. 6 exhibit a well-structured pattern which is assumed to reflect either the distribution of defects in the crystal or the waviness of the outside surface. The first effect indicates that IR light might be scattered at crystal imperfections into the fiber at an angle where total reflection can take place, and this light is accordingly transmitted to the detector. In addition, it is well known that the surface of flexible fibers exhibits a certain waviness, i.e., a periodic variation of its diameter. This effect arises from the pulling process of the fiber and is on the order of a few microns for a 300 μm fiber according to the manufacturer. As a consequence, the angle between the incident light and the surface, and therefore the angle of refraction, varies locally. This also leads to a fraction of light whose incidence angle fulfills the conditions for total reflection at the second interface. Both effects result in an additional radiation density measured at the Si photodetector. Based on the measurements performed, however, the two effects cannot be distinguished.

At the x positions which correspond to the most significant peaks in the spectra, imperfections in the fiber could be observed optically even with the naked eye. The observed structure is quite similar for both illumination angles. For $\gamma = 60°$ the detected radiation density is larger by a factor of 2 than that for $\gamma = 90°$. However, it must be noted here that the corresponding detected radiation density when illuminating the front end of the fiber at 0° was more than a factor of 10^4 higher than the values measured when illuminating the fiber from the side. Hence, the effect of the parasitic radiation which enters the fiber from the side can be assumed to be rather small.

In Fig. 6, the additional radiation density detected using the rigid sensor with the same calibration is also shown. In contrast to the flexible sensor, no x dependence could be observed within the uncertainty band of measurement. For a fixed angle, this effect turns out to be about a factor of 15 smaller than that for the flexible sensor. A corresponding increase of the background signal could therefore not be detected.

In the second experiment the attention has been focused on a comparison of the radiation coupled into the fiber near the tip with the radiation entering the fiber via the front within the effective aperture. Since the former experiment has clarified that the major part of the parasitic transmission enters the fiber near the tip, there was no longer any need for local resolution. The experiment is described in section 3.3 and sketched in Fig. 4. The measured data are graphically represented in Fig. 7 for angles larger than 20°, because smaller angles did not allow proper measurement. The dependence of the parasitic radiation density on the angle γ is shown in units of maximum intensity, i.e., for $\gamma = 0°$. For angles larger than 35°, quite a similar ratio of the parasitic radiation contributions for the flexible and rigid sensor as observed for $\gamma = 90°$ (see also Fig. 5) has been found; the parasitic radiation is about a factor of 5 larger for the flexible sensor.

There arises the question of how this dependence is related to the determination of the effective aperture shown in Fig. 2. Whereas Fig. 2 shows the intensity transmitted within 0° and γ, Fig. 7 illustrates the intensity transmitted within $\gamma - d\gamma$ and $\gamma + d\gamma$, with $d\gamma$ being the variation of the angle. If $d\gamma$ were small enough, Fig. 7 would represent the derivative with respect to the angle of the curve represented in Fig. 2, under the assumption that the radiation bulb would be extended infinitely.

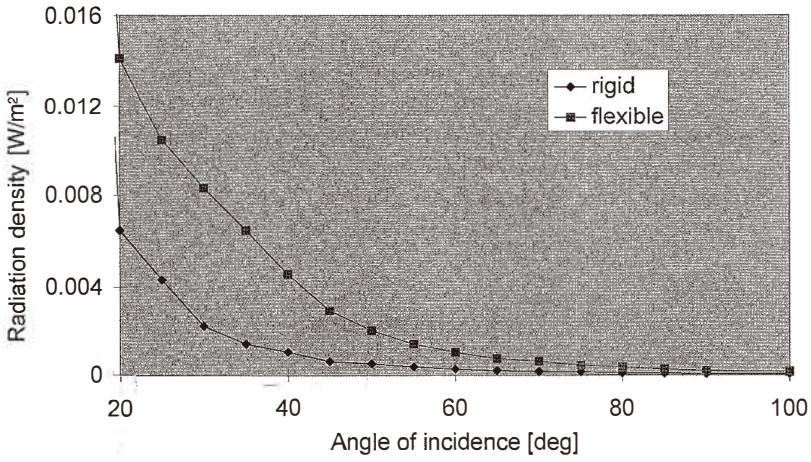

Fig. 7. Measured radiation density versus the angle of incidence γ for the two sensors when illuminating the fiber tip with parallel light.

3.4.4 *Evaluation*

The relatively small amount of radiation which is coupled into the fiber via its side, as perceived in the experiment corresponding to Fig. 6, demonstrates that this effect is negligible when using the flexible fiber as a light pipe sensor. Nevertheless, these observations might be interesting for the study of the defect distribution within the flexible fiber and the angular dependence for scattering at the crystal defects and surface imperfections. The determined difference in the parasitic radiation intensity of a factor of 15 between the flexible and the rigid sensors reflects the well-known fact that the number of crystal imperfections for a flexible sapphire fiber is much higher than for the rigid fiber.

The second experiment revealed, as discussed in section 3.1, that 5% of the intensity transmitted by the flexible sensor has been detected for angles larger than 15°. Since the radiation bulb illuminates the sensor at an angle of 28°, the question of whether this value might be higher for a larger extension of the bulb might arise. Based on Fig. 7, this question can be ignored, since the absorption function becomes very small for angles larger than 30°, compared to smaller angles. If light falls in larger angles —for instance if the fiber is inside a cavity— the contribution of angles larger than 30° can be estimated, with the help of Fig. 7, to be less than 1% of the full intensity. Figure 7 also shows that for angles larger than 30° the absorption for the flexible sensor is 5 times as large as the absorption of the rigid sensor.

Further measurement has shown that there is no influence of different polishing procedures of the sensor surfaces on the observed effects. A rigid sensor fabricated following the technique described in section 3.3 gave the same results as the investigated commercial sensor which has been polished in a different manner by the manufacturer of

these sensors. This indicates that the effect of coupling light from the side is caused not by the structure of the surface but by crystal defects near the tip.

It is assumed that the grinding process itself increases the number of already existing defects at the end of the fiber. This assumption is supported by the fact that there are more defects in a flexible sensor leading also to a larger increase for the flexible type, as observed. A similar phenomenon has also been found for the crystal structure near the surface of polished diamond in pseudopotential calculations.[14]

4. Conclusions

It has been shown that an operational OFT light pipe sensor can be fabricated using a 325 μm flexible sapphire fiber. The results of the characterization tests have shown that this sensor exhibits a high performance for temperature measurements comparable to that of a rigid sensor. Below, the findings of this work are summarized as follows:

Concerning the short-term stability and the limitation in the lower temperature range, an identical behavior is found for the flexible OFT sensor as for a conventional, rigid OFT light pipe sapphire sensor.

A slight difference in the effective aperture between the two sensor types could be identified. The tests show that the rigid sensor detects 90% of the total intensity of emitted radiation by means of an extended source within an angle of 7°, whereas the respective angle for the flexible sensor is determined to be about 11°. Moreover, for a flexible sensor, about 4% is still detected in the area outside of 15°, whereas the rigid sensor detects less than 1%. The local resolution of the sensor, however, is only slightly affected by the slightly enlarged angle of acceptance for the flexible fiber.

Furthermore, off the side of the tip, the contribution of radiation which is coupled into the fiber via the side to the total transmitted radiation intensity is negligible. The regularly transmitted radiation which enters the fiber via the effective aperture of the front is several orders of magnitude larger. Through detailed examination, this effect for a flexible sensor is found to be about 15 times as large as that for the rigid sensor.

Hence, this additional radiation would not falsify a temperature measurement even if the fiber is placed in a cavity with a strong temperature gradient, or is lead through hot zones as, for example, in an engine or combustion experiment.

It is known that the amount of crystal imperfections in a flexible fiber is several orders of magnitude larger than that in a rigid sapphire rod. This, or surface imperfections, can be the cause of the observed difference in the parasitic side radiation off the side of the tip. However, it is assumed that the reason for the difference in the measured effective aperture lies in the much larger number of crystal imperfections in the volume next to the tip for the flexible fiber than those present a priori in the fiber. This rather enlarged number of lattice distortions also scatters light into the angle of acceptance such that it enters the fiber at a larger angle than the effective aperture. Therefore, the angle of acceptance is thought to be effectively enlarged compared to that of the rigid sensor.

A similar well-known effect of diamond polishing, the enlargement of imperfections, is most probably induced by the grinding process of the surface.[14] Hence, when calibrating

a flexible OFT sensor, this slightly enlarged aperture must be taken into account. Using an extended radiation source with homogeneous temperature would be ideal for this purpose.

For application as a control sensor in a high-temperature furnace, the observed difference in the effective aperture is of minor impact. In this case a replacement of a rigid sensor by a flexible one would not result in a performance loss; moreover, the sensor would provide more flexibility concerning routing. Furthermore, when using a flexible OFT sensor for high-precision measurement of temperature fluctuations in a metallic or semiconductor melt, the disturbance of the flow field by the sensor itself is much lower than that by a rigid one.

Acknowledgments

We would like to thank Chuck Schietinger for valuable comments and fruitful discussions, and LUXTRON Inc. for providing us with the bare flexible fibers.

References

1 R. E. Bedford: High-Temp. — High Pressures **4** (1972) 241.
2 R. R. Dils: J. Appl. Phys. **54** (1983) 1198.
3 C. Schietinger: Temperature measurements using optical fibers, in Thermal measurements in Electronics Coolings, ed. K. Azar (CRC Press, Boca Raton, 1997).
4 Ch. Stenzel, P. Dold and K. W. Benz: Rev. Sci. Instr. **67** (1996) 1985.
5 H. E. LeBelle jr.: J. Cryst. Growth **50** (1980) 8.
6 J. A. Harrington, A. G. Standlee, A. C. Pastor and L. G. deShazer: SPIE Proc. **484** (1984) 124.
7 J. J. Fitzgibbon, H. E. Bates, A. P. Pryshlak and J. R. Dugan: SPIE Proc. **2396** (1995) 60.
8 J. J. Fitzgibbon, A. P. Pryshlak and J. R. Dugan: SPIE Proc. **2677** (1996) 35.
9 V. Bhatia, K. A. Murphy, R. G. May, R. O. Claus, T. A. Tran, J. A. Greene and J. E. Coate: High Temp. & Mat. Sc. **35** (1996) 31.
10 A. Wang, S. Gollapudi, R. G. May, K. A. Murphy and R. O. Claus: Smart Mater. Struct. **4** (1995) 147.
11 X. Fang, R. G. May, A. Wang and R. O. Claus: Sensors and Actuators A **44** (1994) 19.
12 Internet homepage of *Saphikon*, Inc.: http://www.saphikon.com
13 R. E. Einziger and J. N. Mundy: Rev. Sci. Instr. **47** (1976) 1547.
14 M. R. Jarvis, R. Perez, F. M. van Bouwelen and M. C. Payne: Phys. Rev. Lett. **80** (1998) 3428.

About the authors

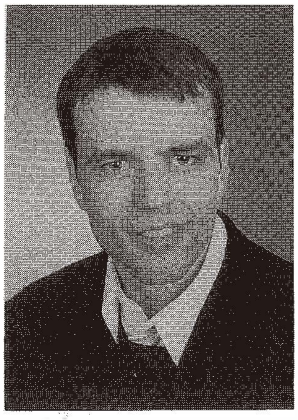

Jörg P. Kottman received the Dipl.-Phys. degree form the Free University of Berlin, Germany in 1997. In January 1998, he joined Dornier GmbH Friedrichshafen to investigate the feasibility of flexible sapphire fibers for high-temperature measurement systems. Since May 1998, he is working for his Ph.D. degree at the Laboratory of Field Theory and Microwave Electronics of the Swiss Federal Institute of Technology (ETH) in Zurich, Switzerland. His interests include the development of computational techniques for optics and the theoretical investigation of the interaction of light with nanostructures.

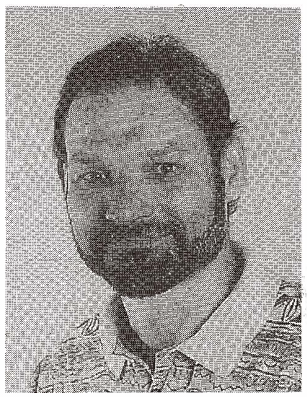

Christian Stenzel received the Ph.D. in Physics from the Free University of Berlin, Germany in 1986. He worked in 1987 as a research associate at the State University of New York (SUNY) at Stony Brook, USA and in 1988, at the Hahn-Meitner-Institut, Berlin in the field of solid-state physics using nuclear methods. In 1989 he joined the Materials Science Department of Dornier GmbH, Friedrichshafen to develop new technologies for materials science experiments under microgravity. His special interests are concentrated on high-temperature measurement techniques, new heater technologies, and diagnostic and stimuli systems.